PAPER

Super-Resolution Time of Arrival Estimation Using Random Resampling in Compressed Sensing

Masanari NOTO[†], **Fang SHANG**[†], **Shouhei KIDERA**[†a)], ***and*** **Tetsuo KIRIMOTO**[†], ***Members***

SUMMARY There is a strong demand for super-resolution time of arrival (TOA) estimation techniques for radar applications that can that can exceed the theoretical limits on range resolution set by frequency bandwidth. One of the most promising solutions is the use of compressed sensing (CS) algorithms, which assume only the sparseness of the target distribution but can achieve super-resolution. To preserve the reconstruction accuracy of CS under highly correlated and noisy conditions, we introduce a random resampling approach to process the received signal and thus reduce the coherent index, where the frequency-domain-based CS algorithm is used as noise reduction preprocessing. Numerical simulations demonstrate that our proposed method can achieve super-resolution TOA estimation performance not possible with conventional CS methods.

key words: *super-resolution TOA estimation, compressed sensing (CS), radar signal processing, random re-sampling*

1. Introduction

Microwave radar provides one of the most useful detection and ranging systems in that it can be used in all weather conditions. In general, the range resolution of radar systems, which is strictly limited by the frequency bandwidth of the transmitted signal, is often insufficient for practical radar applications because of legal regulations or hardware limitations. Thus, super-resolution time of arrival (TOA) estimation methods such as the Capon method and multiple signal classification (MUSIC) method [2], [3] have been attracting attention. The Capon method achieves super-resolution performance with providing scattering coefficient, by suppressing the range sidelobe with the constrained norm power minimization scheme [2]. On the other hand, the MUSIC method exploits the orthogonality between the signal and noise eigenvector correlation matrix, and achieves higher resolution than the Capon method. However, it requires *a priori* knowledge of the number of targets, and it is inherently difficult to obtain the target scattering coefficient [3]. These methods suffer from low resolution and accuracy for separating highly correlated signals, which is an inherent problem in radar signal processing. To achieve accurate separation of highly correlated interference signals, one approach [4] has incorporated maximum likelihood independent component analysis (MLICA) into the MUSIC method; the effectiveness of this approach has been experimentally confirmed. However, conventional methods manifest limited range resolution when separating highly correlated signals, even after tuning parameters.

Given to this background, this paper introduces a compressed-sensing (CS)-based approach with random resampling to address the TOA estimation issue. CS is widely recognized as one of the most powerful means of solving underdetermined and ill-posed inverse problems with constrained l_1 norm minimization [5]. It requires only one assumption that the spatial or temporal distribution of targets should be sparse compared to the total sampled area [6]. There are intensive researches for CS-based signal processing for various applications. Specifying to the radar applications, the CS method has been demonstrated that it achieved both a relatively lower sampling rate and high-resolution property in such as synthetic aperture radar (SAR) based image reconstruction problem [7]–[9], the TDOA (Time Difference of Arrival) discrimination issues [10], [11] and the spectrum reconstruction schemes [12], [13]. However, it has been reported that the original CS algorithm suffers from inaccuracy if the return signals are strongly contaminated by noise [6], especially when highly correlated target signals are also closely located within the theoretical range resolution. While there are some studies based on the Bayesian CS algorithm for TOA estimation [14], which improves TOA estimation accuracy by employing a stochastic model of signal and noise, this kind of method requires accurate signal and noise probability models, which is not flexible to various observation situations.

There are some studies that random resampling can alleviate the problem of a highly coherent observation matrix and can help separate highly correlated radar responses [15]. To reduce the coherence index denoted in [16], this research introduces the statistical incorporation of multiple outputs of random re-sampling based CS algorithm, with appropriate noise reduction filter as frequency-domain-based CS algorithm by exploiting *a priori* knowledge of a target response in both time and frequency domains, because the frequency spectrum of received signal itself could be regarded as sparse by using zero-padding process. Numerical simulations verify that the proposed method offers better resolution in noisy conditions than the conventional methods, including the original CS method.

This paper is organized as follows. Section 2 describes the system model in radar system considered in this research. Section 3 briefly introduces conventional approaches such as MUSIC, MLICA-based MUSIC, and the

Manuscript received August 22, 2017.
Manuscript revised November 24, 2017.
Manuscript publicized December 18, 2017.

[†]The authors are with Graduate School of Informatics and Engineering, University of Electro-Communications, Tokyo, 182-8585 Japan.
a) E-mail: kidera@ee.uec.ac.jp

DOI: 10.1587/transcom.2017EBP3324

original CS method. Section 4 introduces the proposed approach using a random resampling and frequency-domain-based CS method and describes the procedures. Section 5 presents the result of our numerical simulation and demonstrates the effectiveness of the proposed method when applied to a typical TOA problem.

2. System Model

Figure 1 shows the system model. It assumes that a monostatic radar system and that the temporal distribution of multiple-point scatterers can be expressed as;

$$\theta(t) = \sum_{i=1}^{N_T} a_i \delta(t - \tau_i), \tag{1}$$

where $\delta(*)$ is Dirac's delta function, a_i and τ_i are the i-th scattering coefficients of scatterers and time delay, respectively, and N_T is the number of targets. The receiving signal $x(t)$ is expressed as;

$$x(t) = \int_{-\infty}^{\infty} \theta(t - \tau) h(\tau) d\tau + e(t), \tag{2}$$

where $h(t)$ is the transmitting signal and $e(t)$ is the thermal noise at the receiver. The discrete form in Eq. (2) is expressed as;

$$\boldsymbol{x} = \boldsymbol{\Phi}\boldsymbol{\theta} + \boldsymbol{e}, \tag{3}$$

where

$$\boldsymbol{\theta} = [\theta(-K\Delta t_{\mathrm{AD}}), \theta((-K+1)\Delta t_{\mathrm{AD}}), \cdots, \theta(N\Delta t_{\mathrm{AD}})]^T, \tag{4}$$

$$\boldsymbol{\Phi} = \begin{pmatrix} h(K\Delta t_{\mathrm{AD}}) & \cdots & h(0) & 0 & \cdots & \cdots & 0 \\ 0 & h(K\Delta t_{\mathrm{AD}}) & \cdots & h(0) & 0 & \cdots & 0 \\ & & & \ddots & & & \\ 0 & \cdots & \cdots & 0 & h(K\Delta t_{\mathrm{AD}}) & \cdots & h(0) \end{pmatrix}, \tag{5}$$

$$\boldsymbol{x} = [x(\Delta t_{\mathrm{AD}}), \cdots, x(N\Delta t_{\mathrm{AD}})]^T, \tag{6}$$

$$\boldsymbol{e} = [e(\Delta t_{\mathrm{AD}}), \cdots, e(N\Delta t_{\mathrm{AD}})]^T, \tag{7}$$

where K and N denote the numbers of data length of the transmitting signal and receiving signal, respectively. Δt_{AD} denotes the sampling interval of A/D conversion. $\boldsymbol{\Phi}$ is the observation matrix, which in typical TOA estimation by radar systems, guarantees the assumption that $N_T \ll N$, which corresponds to the sparse representation.

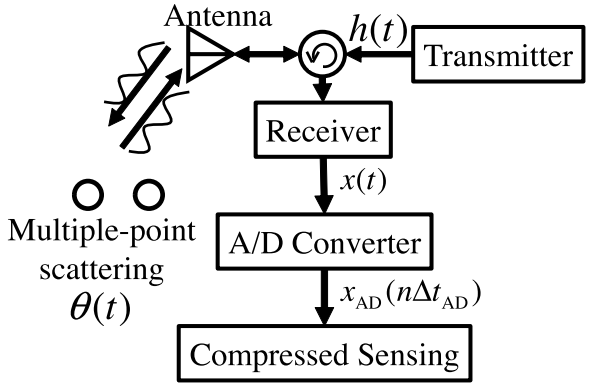

Fig. 1 System model.

3. Conventional Method

This section briefly describes numerous conventional TOA estimation methods: MUSIC, MLICA-based MUSIC, and the original CS.

3.1 MUSIC Method

The MUSIC method, which has been widely used as a super-resolution TOA technique, employs eigenvectors determined by a noise subspace decomposed from a correlation matrix of the assumed transfer function in the frequency domain. This can be expressed as;

$$Z(n\Delta\omega) = \frac{X(n\Delta\omega)}{H(n\Delta\omega)}, \tag{8}$$

where $X(n\Delta\omega)$ and $H(n\Delta\omega)$ are discrete forms after applying Fourier transform to $\boldsymbol{x}$ and $\boldsymbol{h}$, respectively, and $\Delta\omega$ is the sampling interval of the angular frequency domain. The correlation matrix of $\boldsymbol{Z}$ is calculated as;

$$\boldsymbol{R} = \sum_{n=1}^{N-M+1} \boldsymbol{Z}_n \boldsymbol{Z}_n^H, \tag{9}$$

where $\boldsymbol{Z}_n = [Z(n\Delta\omega), \cdots, Z((n+M-1)\Delta\omega))]^T$, ^{H} denotes the Hermitian transpose, M denotes the dimension of the subspace in the frequency domain, and M is satisfied with $M < N$. To suppress correlated interference signals, frequency averaging is used in the frequency correlation matrix. The output of MUSIC is expressed as;

$$\theta_{\mathrm{music}}(t) = \frac{\boldsymbol{a}^H(t)\boldsymbol{a}(t)}{\boldsymbol{a}^H(t)\boldsymbol{E}_n\boldsymbol{E}_n^H\boldsymbol{a}(t)}, \tag{10}$$

where $\boldsymbol{a}(t) = [\exp(-\mathrm{j}\Delta\omega t), \cdots, \exp(-\mathrm{j}M\Delta\omega t)]^T$ is a steering vector, $\boldsymbol{E}_n$ comprises the eigenvectors of $\boldsymbol{R}$, which should correspond to the noise component. A disadvantage of this method is that it requires *a priori* information of the number of targets, and thus, it cannot directly derive the scattering coefficient.

3.2 MLICA-Based MUSIC Method

When compared with MUSIC separation, to achieve more accuracy and higher resolution, MLICA-based preprocessing has been introduced [4]. To obtain multiple received signals in a single observation, this method generates multiple frequency-shifted signals known as quasi multiple channels. A quasi multiple channels $\boldsymbol{Z}$ is defined as;

$$\begin{aligned} &\boldsymbol{Z} = [\boldsymbol{Z}_1, \boldsymbol{Z}_2, \ldots, \boldsymbol{Z}_{L'}]^{\mathrm{T}}, \\ &\boldsymbol{Z}_n = [Z(n\Delta\omega), Z((n+1)\Delta\omega), \ldots, Z((n+Q-L')\Delta\omega)] \\ &\qquad\qquad (n = 1, 2, \ldots, L'), \end{aligned} \tag{11}$$

where L' is the number of quasi multiple channels and Q denotes the number of available frequency indexes. These signals can be decomposed into uncorrelated signals using a principal component analysis (PCA) as;

$$\boldsymbol{Z}^{\mathrm{P}} = \boldsymbol{M}\boldsymbol{Z}, \tag{12}$$

where $\boldsymbol{M}$ is a whitening matrix determined by PCA. Each signal is decomposed by MLICA using a probability density function (PDF) of complex sinusoidal signals [17]. The separated signal $\hat{\boldsymbol{Z}}$ is formulated as;

$$\hat{\boldsymbol{Z}} = \boldsymbol{W}\boldsymbol{Z}^{\mathrm{P}}, \tag{13}$$

where $\boldsymbol{W}$ is determined by MLICA-based optimization [17]. The effectiveness of this method has been experimentally verified, and it has been shown to achieve greater accuracy and higher resolution than MUSIC. However, its TOA resolution is still limited.

3.3 Original Compressed Sensing

CS-based signal decomposition is an alternative approach to super-resolution. CS-based TOA estimation only assumes the sparseness of the target distribution in the time domain [6]. The temporal distribution of the target is determined as;

$$\hat{\boldsymbol{\theta}} = \arg\min_{\boldsymbol{\theta}} \left(\|\boldsymbol{x} - \boldsymbol{\Phi}\boldsymbol{\theta}\|_2^2 + \lambda \|\boldsymbol{\theta}\|_1 \right), \tag{14}$$

where λ is a regularization coefficient and $\|\boldsymbol{v}\|_p = (|v_1|^p + \cdots + |v_N|^p)^{\frac{1}{p}}$ denotes l_p norm. The second term in the temporal distribution of the target specifies the sparseness. Although it has been reported that the original CS method can achieve higher resolution than the conventional MUSIC-based methods, it suffers from inaccuracy or lower resolution in noise environments and when signals are highly correlated.

4. Proposed Method

To overcome the problems of the original CS method, this research investigated the use of random resampling technique and frequency-domain-based CS for noise reduction. Here, the difficulty index for the decomposition problem is derived by Eq. (3), and $\mu(\boldsymbol{\Phi})$ is introduced as;

$$\mu(\boldsymbol{\Phi}) = \max_{1 \le i < j \le N_0} \frac{|\boldsymbol{\phi}_i^H \boldsymbol{\phi}_j|}{\|\boldsymbol{\phi}_i\|_2 \|\boldsymbol{\phi}_j\|_2}, \tag{15}$$

where $\boldsymbol{\phi}_i$ is the i-th column vector of the observation matrix $\boldsymbol{\Phi}$ and N_0 is the number of the column vector. This index is known as the coherence index, and several previous studies have shown that $\mu(\boldsymbol{\Phi})$ is useful in assessing the difficulty of a CS reconstruction problem [16]. It has been demonstrated in [15] that $\mu(*)$ can be reduced using a random resampling technique that applies downsampling with a randomly determined interval. Figure 2 shows an example of the resampling process used in this research.

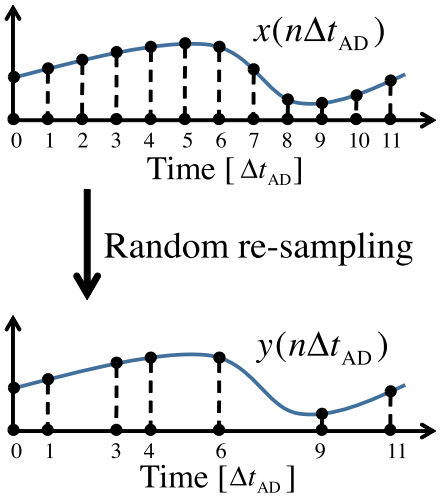

Fig. 2 Scheme of random re-sampling.

By exploiting *a priori* knowledge of frequency range of target signal, the proposed method introduces the noise reduction pre-processing with CS based spectrum reconstruction as;

$$\hat{\boldsymbol{X}}_m = \arg\min_{\boldsymbol{X}_m} \left(\|\boldsymbol{y}_m - \boldsymbol{\Psi}\boldsymbol{F}^{-1}\boldsymbol{X}_m\|_2^2 + \beta \|\boldsymbol{X}_m\|_1 \right), \tag{16}$$

where $\boldsymbol{X}_m$ is the Fourier transform of receiving signal, $\boldsymbol{F}^{-1}$ is the inverse Fourier transform matrix, $\boldsymbol{\Psi}$ is the random re-sampling matrix in the time domain, $\boldsymbol{y}_m$ denotes the receiving signal in randomly resampled in the same manner, m denote the index number of the random resampling pattern, and β is a regularization coefficient. Since a random-resampling process generates unevenly sampled data in time domain, then, the traditional noise-reduction filter (e.g. matched filter or BPF filter) is hardly applied using the usual DFT or FFT due to unsatisfying the orthogonality of the basis functions. However, Eq. (16) easily forms an appropriate filter even for unevenly sampled data, while non-uniform sampled FFT requires much complicated process [18]. The another motivation for applying Eq. (16) is not for the frequency spectrum reconstruction of signal, but for the noise-reduction, where the white Gaussian noise components outside the signal frequency range would be effectively eliminated.

Note that, the CS process in the time domain reconstructs the temporal distribution $\boldsymbol{\theta}$ as in Eq. (14), where the sparsity in the time domain is guaranteed because $\boldsymbol{\theta}$ is expressed in Eq. (1). On the contrary, the CS process in the frequency domain reconstructs the frequency expression of the received signal $\boldsymbol{x}$ (not $\boldsymbol{\theta}$) as in Eq. (16), where $\boldsymbol{x}$ is expressed as the convolution between $\boldsymbol{\theta}$ and the transmitted signal $h(t)$ as in Eq. (2). Thus, the sparsity in the frequency domain of $\boldsymbol{X}$ is also guaranteed by not using the receiver with a redundant bandwidth, but applying the zero-padding process in the frequency domain, because the frequency range of received signal is determined by that of the transmitted signal

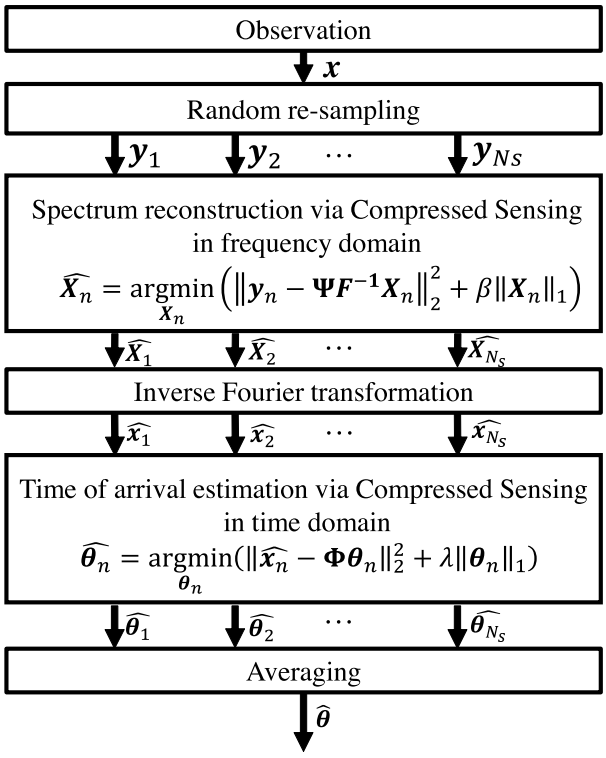

Fig. 3 Flowchart of the proposed method.

as in Eq. (2). Then, the proposed method requires the condition that the bandwidth of the receiver should be larger than that of the received signals, which is common condition in the other conventional methods. While this kind of signal processing requires *a priori* knowledge of the maximum frequency of received signals, in most cases of radar measurement, the received signal model as in Eq. (2) is well-established, and then, the dominant frequency band of received signals can be correctly retrieved from that of the assumed transmitted signal. After this process, the reconstructed signal $\hat{x}_n$, which is obtained by applying inverse Fourier transform to $\hat{X}_n$, is assessed by CS in the time domain using Eq. (14), and the target distribution $\hat{\boldsymbol{\theta}}_n$ is generated for each random resampling pattern.

To obtain a statistically meaningful output, in this research, we introduced the averaging of multiple outputs calculated by different resampling patterns as;

$$\hat{\boldsymbol{\theta}} = \frac{\sum_{n=1}^{N_s} \hat{\boldsymbol{\theta}}_n}{N_s}, \tag{17}$$

where N_s denotes the number of random resampling patterns. The procedure used in the proposed method is as follows:

Step 1)
$\boldsymbol{y}_n$ is obtained for the n-th random resampling pattern of the receiving signal $\boldsymbol{x}$.

Step 2)
CS is applied in the frequency domain, and $\hat{\boldsymbol{X}}_n$ is reconstructed using Eq. (16).

Step 3)
The target distribution $\hat{\boldsymbol{\theta}}_n$ is reconstructed using time domain CS with the reconstructed signal vector, which is the inverse Fourier transform of $\hat{\boldsymbol{X}}_n$.

Step 4)
Steps 1) - 3) are repeated N_s times, where the pattern of random resampling is changed.

Step 5)
The averaged reconstructed signal $\hat{\boldsymbol{\theta}}$ is derived.

Figure 3 shows a flowchart of the proposed method.

5. Performance Evaluation Using Numerical Simulation

This section describes the performance of the conventional and proposed methods is evaluated through numerical simulations. The transmitting signal is a chirp-modulated pulse, expressed as;

$$h(t) = \mathrm{rect}\,(t; K) \exp\left(\mathrm{j}\alpha t^2\right), \tag{18}$$

$$\mathrm{rect}\,(t; K) = \begin{cases} 1 & (0 \le t \le K) \\ 0 & (\text{otherwise}), \end{cases} \tag{19}$$

where α is the chirp rate and K is the number of pulse length. Receiver thermal noise, treated as complex white Gaussian noise, is added to the receiving signal. The signal-to-noise ratio (SNR) is defined as the time averaged power ratio between signal and noise after applying a bandpass filter (BPF) determined by the bandwidth of the transmitting signal. Table 1 shows parameters used in the numerical simulation, where $\Delta\tau_0$ denotes the time resolution determined by the frequency bandwidth of the transmitting signal. Figures 4 and 5 show the received signal in the time domain as $\boldsymbol{x}$ and in the frequency domain as $\boldsymbol{X}$, before and after zero-padding processing in frequency domain, respectively. As shown in these figures, the dominant ratio of the spectrum of the received signal as $\boldsymbol{X}$ decreases in the frequency domain, compared with that before zero-padding process, which corresponds to the oversampling process in the time domain. Note that, the zero padding process expands the frequency range in Fourier analysis, while the frequency range of the received signal is invariant, and this process brings us to more suitable situation for the sparsity in the frequency domain. For the CS optimization, the interior algorithm [19] is used in this case, by considering the balance between optimization accuracy and computational cost. Figure 6 shows the outputs of the conventional MUSIC, MLICA-based MUSIC, original CS, and proposed methods, in the noiseless case. It can be seen that every method can separate two completely correlated target signals, the temporal interval of which is set as $\Delta\tau_0/8$. Figure 7 shows the output of each method in noise case with an SNR of 15 dB with the same noise pattern. The conventional MUSIC method, MLICA based MUSIC method and CS method fail to separate the two targets under these conditions. In contrast, in the lowest side of Fig. 7 shows that the proposed method accurately reconstructed both targets. This results denotes that

Table 1 Parameters used in numerical simulation.

Number of targets	2
Temporal interval of two targets	$\Delta\tau_0/8$
Sampling rate at time domain	$\Delta\tau_0/16$
Regularization coefficients λ	0.5
Regularization coefficients β	0.01
Number of pulse lengths	$16\Delta\tau_0$
Number of signal lengths	512
Number of random re-sampled signal lengths	256
Number of random re-sampling patterns N_s	5

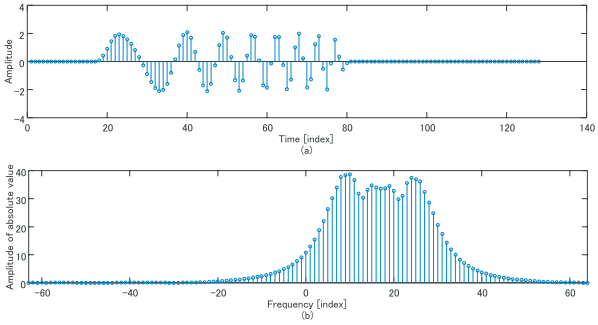

Fig. 4 Received signal before the zero-padding process in the frequency domain (corresponding to oversampling process in the time domain). (a): in the time domain. (b): in the frequency domain.

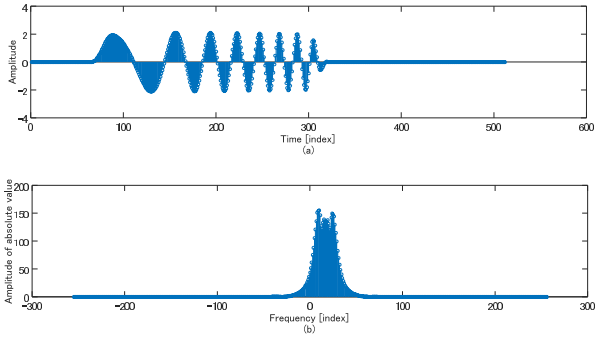

Fig. 5 Received signal after the zero-padding process in the frequency domain (corresponding to oversampling process in the time domain). (a): in the time domain. (b): in the frequency domain.

Table 2 Comparison of $\mu(\mathbf{\Phi})$ for each method.

	$\mu(\mathbf{\Phi})$
Original CS	1.0000
Proposed method	0.9992

our method offers 8 times improvement over the theoretical TOA resolution denoted by $\Delta\tau_0$.

To evaluate another aspect of performance, we introduce the coherence index $\mu(\mathbf{\Phi})$, given by Eq. (15). Table 2 shows the coherence index $\mu(\mathbf{\Phi})$ of both the original CS and proposed methods. Here, to calculate $\mu(\mathbf{\Phi})$ in the proposed method, we assume the equivalent transmitted signal sequences as $\boldsymbol{h}'$ in Eq. (5). Here, a signal after re-sampling and CS based spectrum reconstruction process (shown in the flowchart as Fig. 3,) is introduced as $\hat{\boldsymbol{x}}$ assuming noiseless situation. In this case, the relationship $\hat{\boldsymbol{x}} = \boldsymbol{h}' * \boldsymbol{\theta}_{\text{true}}$ holds,

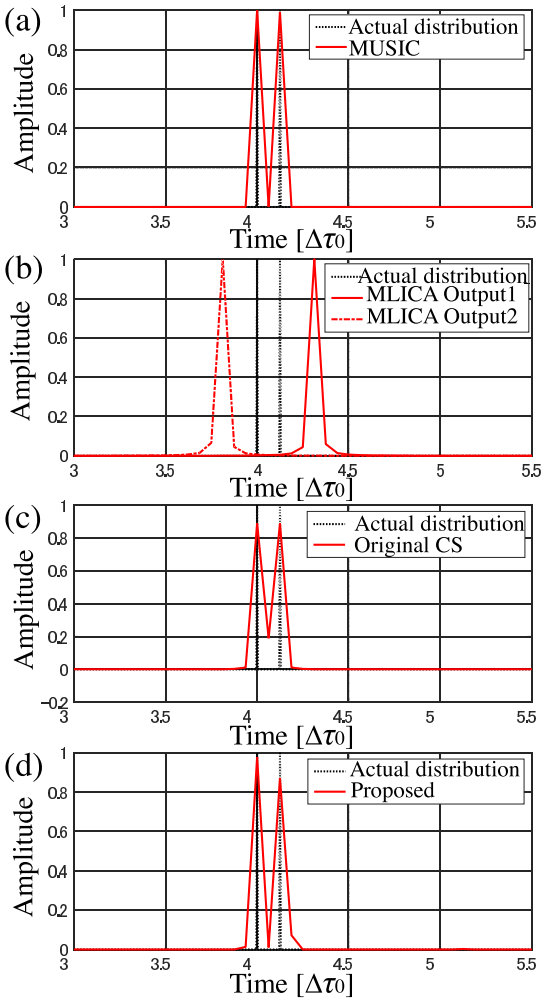

Fig. 6 Outputs of each method in noiseless ((a): the conventional MUSIC, (b): the MUSIC with MLICA, (c): the original CS, (d): the proposed methods).

where $\boldsymbol{\theta}_{true}$ denotes an actual target distribution. Then, $\boldsymbol{h}'$ is derived from the above relationship by the inverse decomposition operation. Finally, $\mathbf{\Phi}$ for the proposed method is re-defined by $\boldsymbol{h}'$ in Eq. (5). This table demonstrates that the proposed method shows a slightly reduced the coherence index $\mu(\mathbf{\Phi})$ but strongly improved separation performance.

Next, the performance index of each method is statistically compared. Here, the error of TOA estimation ϵ is defined as

$$\epsilon = \sqrt{\frac{\|\hat{\boldsymbol{\theta}} - \boldsymbol{\theta}_{\text{True}}\|_2^2}{N'}}, \tag{20}$$

where $\boldsymbol{\theta}_{\text{True}}$ and $\boldsymbol{\theta}$ denote the actual and estimated distribution of scattering coefficients. For example, the two impulse signals in Fig. 6 is recognized as $\boldsymbol{\theta}_{\text{True}}$, each of which has a finite scattering coefficient. N' is the number of data length of the target distribution. Figure 8 plots the median value and interquartile range (IQR) of each method ϵ versus the SNR in each methods. Note that, this evaluation does not need a judgment whether each method estimates the number

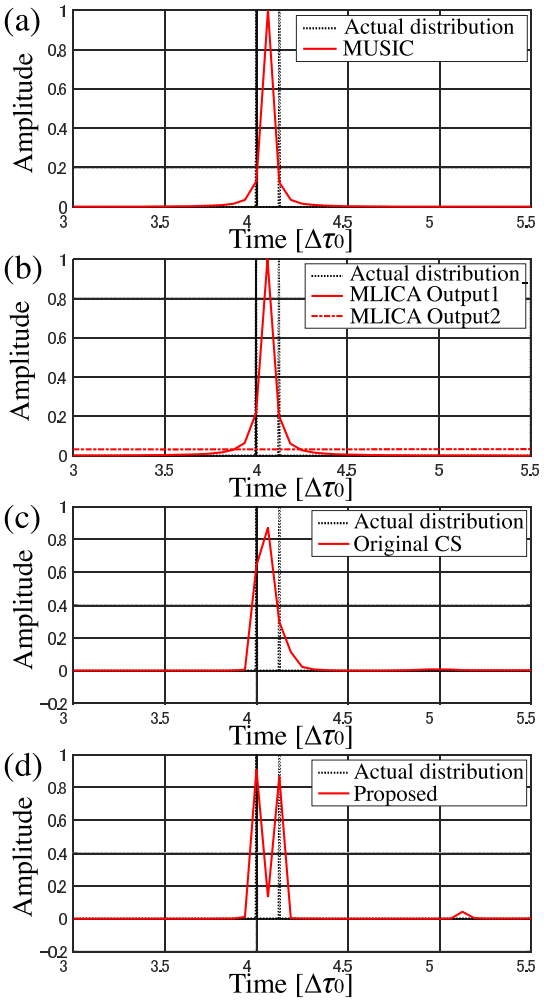

Fig. 7 Outputs of each method at SNR=15 dB((a): the conventional MUSIC, (b): the MLICA based MUSIC, (c): the original CS, (d): the proposed methods).

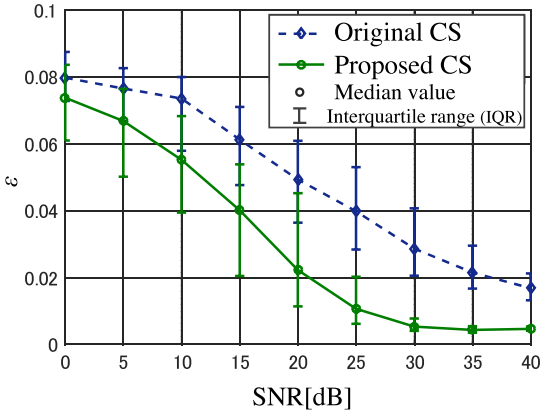

Fig. 8 Median and IQR of ϵ versus SNR for each method.

of arrived signals, because $\boldsymbol{\theta}$ expresses a temporal distribution of scattering coefficient. The noise pattern is changed 100 times. Figure 8 shows that under noise condition, the proposed method demonstrated the highest TOA estimation

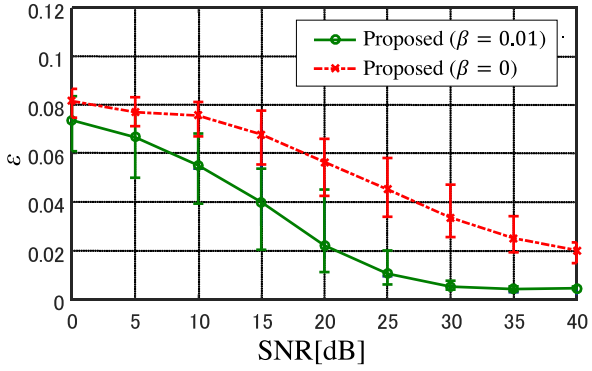

Fig. 9 Reconstruction accuracy comparison for the proposed CS method with ($\beta = 0.01$) and without ($\beta = 0$) frequency domain based CS filter for each SNR. Error bar denotes IQR and each point shows median of errors.

accuracy. In addition, we investigate the effectiveness of noise-reduction filter based on the frequency domain based CS algorithm as in Eq. (16). Figure 9 shows the reconstruction accuracy comparison for the proposed method between with ($\beta = 0.01$) and without ($\beta = 0$) frequency domain based CS filter. This figure demonstrates that the frequency-domain based CS algorithm is effective as noise reduction filter, even if the sparseness in the frequency domain is assumed, and upgrades the reconstruction accuracy in any SNR situations. This result denotes that the sparse regularization in the frequency domain effectively contributes the noise-reduction, where the original target response should be maintained. Note that, since there are many delicately designed filters for noise-reduction, it is our future work to implement such filters using non-uniform FFT algorithm [18].

It should be noted that the conventional MUSIC and MLICA based MUSIC are difficult to evaluate by using ϵ, because these methods cannot retain the scattering coefficient in TOA estimation. This is because the MUSIC based approach is based on the decomposition exploiting the orthogonality to noise components (not including signal amplitude information), and it cannot provide a scattering coefficient of target, directly. To compare the performance of these methods, a separation rate is introduced based on the probability of achieving successful separation. Successful separation is defined as satisfying two conditions: the number of local maximum from the estimated TOA matched the actual number of targets and all TOA errors fell within $\Delta\tau_0$. Figure 10 plots the separation ratio versus the SNR and demonstrates the significant superiority of the separation ratio achieved by the proposed method compared with the original CS, MUSIC and MLICA-based MUSIC approaches. Table 3 shows the calculation time for each method using an Intel(R) Xeon(R) E5-1620 3.60 GHz processor. The proposed method takes time more 2.7×10^3 times than the conventional MUSIC method, and 1.4 times than the original CS. This is because, the proposed method introduces CS algorithm twice.

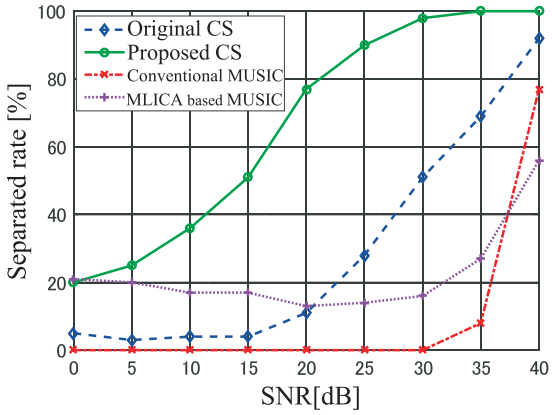

Fig. 10 Separation rate versus SNR for each method.

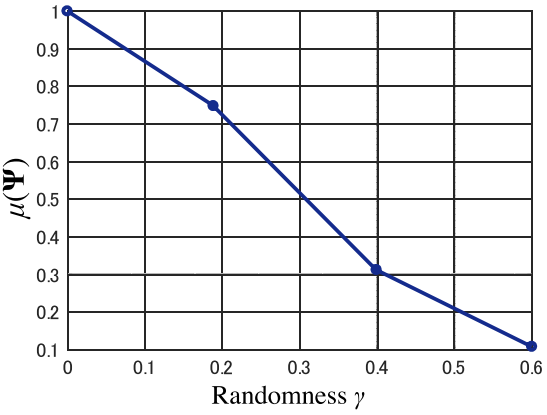

Fig. 11 Coherence index $\mu(\mathbf{\Psi})$ versus randomness.

Table 3 Comparison of calculation times required in each method.

Conventional MUSIC	9.1 ms
MLICA based MUSIC	0.6 s
Original CS	17.2 s
Proposed method	25.0 s

5.1 Random Resampling Effect Analysis

To investigate the effect of random resampling, we first investigated the coherence index $\mu(\mathbf{\Psi})$ under random and periodic resampling. Here, the randomness of the resampling γ is defined as;

$$\gamma = \sum_{n=1}^{N'-1} \frac{|\Delta_{n+1} - \Delta_n|}{N}, \tag{21}$$

where N and N' denotes the numbers of data length for the receiving signal and randomly resampled signal, respectively, and Δ_n is the n-th resampling interval. If $\gamma = 0$, the resampling must be periodic. Figure 11 shows the coherence index $\mu(\mathbf{\Psi})$ for, random and periodic re-sampling. This shows that random resampling effectively can retain the coherence index $\mu(\mathbf{\Psi})$, which is expected achieved more accurate signal reconstruction.

Figure 12 plots the TOA estimation accuracy as the SNR versus ϵ in each sampling method, where the simulation parameters are assumed as in Table 1. The both numbers of periodical and random resampling are 256, while that of full sampling is 512. In the random-resampling case, $\gamma = 0.6$ is set. As shown in Fig. 12, random resampling is shown to have superior reconstruction accuracy than periodic resampling and even full periodic sampling. In particular, the superiority to full periodic sampling case ($\gamma = 1.0$) denotes that, in the case of highly correlated signal decomposition, the lower coherence index $\mu(\mathbf{\Phi})$ has more contribution to the reconstruction accuracy as far as the average interval of random resampling (around $\Delta\tau_0/8$) satisfies the Nyquist condition, namely, the over-sampled data has less contribution to such signal decomposition case. This confirms the more accurate reconstruction of the receiving signal when using the frequency-based CS method with random resampling.

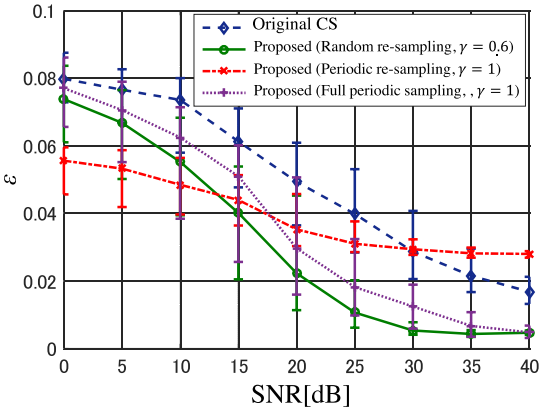

Fig. 12 Median and IQR of ϵ versus SNR for each sampling pattern.

6. Conclusions

This paper proposed a super-resolution TOA estimation method using CS that exploits the features of the transmitted signal through the use of random resampling and frequency domain CS. Conventional MUSIC-based methods and the original CS-based TOA estimation methods suffer from serious inaccuracy and reduced TOA resolution in low SNR environments. In contrast, the proposed method is able to provide super-resolution TOA estimation even in noisy conditions because of improved coherence index, and it achieves 8 times improvement over the theoretical TOA resolution limit denoted as $\Delta\tau_0$, even at very low SNR situations.

References

[1] E. Cook, "Pulse compression-key to more efficient radar transmission," Proc. IRE vol.48, no.3, pp.310–316, March 1960.
[2] J. Capon, "High-resolution frequency-wavenumber spectrum analysis," in Proc. IEEE, vol.57, no.8, pp.1408–1418, Aug. 1969.
[3] H. Nakahara, N. Kikuma, and N. Inagaki, "Signal separation of indoor/pico-cell multipath waves using FFT-MUSIC with triangular antenna array," Proc. ISAP 96, pp.1085–1088, Sept. 1996.

[4] T. Okano, S. Kidera, and T. Kirimoto, "Super resolution TOA estimation algorithm with maximum likelihood ICA based preprocessing," IEICE Trans. Commun., vol.E96-B, no.5, pp.1194–1201, May 2013.
[5] D.L. Donoho, "Compressed sensing," IEEE Trans. Inf. Theory, vol.52, no.4, pp.1289–1306, April 2006.
[6] M.A. Herman and T. Strohmer, "High-resolution radar via compressed sensing," IEEE Trans. Signal Process., vol.57, no.6, pp.2275–2284, June 2009.
[7] R. Baraniuk and P. Steeghs, "Compressive radar imaging," IEEE Proc. 2007 IEEE Radar Conference, pp.128–133, 2007.
[8] V.M. Patel, G.R. Easley, D.M. Healy, Jr., and R. Chellappa, "Compressed synthetic aperture radar," IEEE J. Sel. Topics Signal Process., vol.4, no.2, pp.244–254, April 2010.
[9] S. Camlica, H.E.G. Aselsan, and A.C. Gurbuz, "Analysis of sparsity based joint SAR image reconstruction and autofocus techniques," IEEE Proc. Compressed Sensing Theory and its Applications to Radar, Sonar and Remote Sensing (CoSeRa), 2015 3rd International Workshop on, pp.99–103, June 2015.
[10] J. Schmitz, R. Mathar, and D. Dorsch, "Compressed time difference of arrival based emitter localization," IEEE Proc. Compressed Sensing Theory and its Applications to Radar, Sonar and Remote Sensing (CoSeRa), 2015 3rd International Workshop on, pp.263–267, June 2015.
[11] Y.T. Chan, F. Chan, S. Rajan, and B.H. Lee, "Direct estimation of time difference of arrival from compressive sensing measurements," IEEE Proc. Compressed Sensing Theory and its Applications to Radar, Sonar and Remote Sensing (CoSeRa), 2015 3rd International Workshop on, pp.273–276, June 2015.
[12] M. Bertocco, G. Frigo, and C. Narduzzi, "High-accuracy frequency estimation in compressive sensing-plus-DFT spectral analysis," IEEE Proc. 2015 IEEE International Instrumentation and Measurement Technology Conference (I2MTC), pp.1668–1671, May 2015.
[13] Q. Hou, S. Su, and Z. Chen "Design of digital receiver for ISAR radar based on compressed sampling," IEEE Proc. European Radar Conference (EuRAD), 2014 11th, pp.93–96, Oct. 2014.
[14] C.K. Sung, F. de Hoog, Z. Chen, P. Cheng, and D. Popescu, "Time of arrival estimation and interference mitigation based on Bayesian compressive sensing," IEEE Proc. 2015 IEEE International Conference on Communications (ICC), pp.4612–4617, June 2015.
[15] E.J. Candes and M.B. Wakin, "An introduction to compressive sampling," IEEE Signal Process. Mag., vol.25, no.2, pp.21–30, 2008.
[16] T. Joel and S.J. Wright, "Computational methods for sparse solution of linear inverse problems," Proc. IEEE, vol.98, no.6, pp.948–958, 2010.
[17] T. Okano, S. Kidera, and T. Kirimoto, "MLICA-based separation algorithm for complex sinusoidal signals with PDF parameter optimization," IEICE Trans. Commun., vol.E95-B, no.11, pp.3556–3562, Nov. 2012.
[18] L. Greengard and J. Lee, "Accelerating the nonuniform fast fourier transform," Society for Industrial and Applied Mathematics Review, vol.46, no.3, pp.443–454, 2004.
[19] R.A. Waltz, J.L. Morales, J. Nocedal, and D. Orban, "An interior algorithm for nonlinear optimization that combines line search and trust region steps," Math. Program., vol.107, no.3, pp.391–408, 2006.

Masanari Noto received the B.E. degree in Mechanical Engineering and Intelligent Systems from The University of Electro Communications in 2014. He is currently studying M.E. degree in Mechanical Engineering and Intelligent Systems at the Graduate School of Informatics and Engineering, University of Electro-Communications.

Fang Shang received the B.S. and M.S. degree in electrical engineering and automation from Harbin Institute of Technology, China, in 2009 and 2011. She received the Ph.D. degree in electrical engineering and information systems from The University of Tokyo, Japan, in 2014. She is an Assistant Professor in the Graduate School of Informatics and Engineering, University of Electro-Communications, Japan. Her current research interest is in the signal and imaging processing for the polarimetric SAR and the UWB radar.

Shouhei Kidera received his B.E. degree in Electrical and Electronic Engineering from Kyoto University in 2003 and M.I. and Ph.D. degrees in Informatics from Kyoto University, Kyoto, Japan, in 2005 and 2007, respectively. He has been with Graduate School of Informatics and Engineering, the University of Electro-Communications, Tokyo, Japan, since 2009, and is currently an Associate Professor. He has been stayed at the Cross-Disciplinary Electromagnetics Laboratory in the University of Wisconsin Madison as the visiting researcher in 2016. His current research interest is in advanced radar signal processing or electromagnetic inverse scattering issue for ultra wideband (UWB) three-dimensional sensor or bio-medical applications. He was a recipient of the 2012 Ando Incentive Prize for the Study of Electronics, 2013 Young Scientist's Prize by the Japanese Minister of Education, Culture, Sports, Science and Technology (MEXT), and 2014 Funai Achievement Award. He is a member of the Institute of Electronics, Information, and Communication Engineers of Japan (IEICE), and the Institute of Electrical and Electronics Engineering (IEEE).

Tetsuo Kirimoto received the B.S. and M.S. and Ph.D. degrees in Communication Engineering from Osaka University in 1976, 1978 and 1995, respectively. During 1978–2003 he stayed in Mitsubishi Electric Corp. to study radar signal processing. From 1982 to 1983, he stayed as a visiting scientist at the Remote Sensing Laboratory of the University of Kansas. From 2003 to 2007, he joined the University of Kitakyushu as a Professor. Since 2007, he has been with the University of Electro-Communications, where he is a Professor at the Graduate School of Informatics and Engineering. His current study interests include digital signal processing and its application to various sensor systems. Prof. Kirimoto is a senior member of IEEE and a member of SICE (The Society of Instrument and Control Engineers) of Japan.